Partial Wave Analysis of the Experimental Photomeson Cross Sections*

K. M. WATSON,† *University of Wisconsin, Madison, Wisconsin*

AND

J. C. KECK, A. V. TOLLESTRUP, AND R. L. WALKER, *California Institute of Technology, Pasadena, California*

(Received August 15, 1955)

The experimental data concerning photopion production is studied for photon energies below 400 Mev. The data are analyzed in terms of S- and P-waves of the final pion-nucleon system, and an indication is obtained of the importance of higher partial waves. The "(3,3) state" matrix elements seem to be significantly larger than the other P-wave matrix elements at energies below 400 Mev, but not at higher energies. The energy dependence of the various partial waves can be understood on the basis of rather general arguments.

In addition to the S-wave and "enhanced" P-wave matrix elements involving the (3,3) state, first order correction terms from the other, nonenhanced P-waves are included in the theory. This provides a fairly satisfactory description, for energies below about 350 Mev, of the positive and neutral photopion cross sections in hydrogen, and of the ratio of π^- to π^+ production from deuterium.

1. INTRODUCTION

THE purpose of the present work is to discuss on rather general grounds the interpretation of the experimental photomeson cross sections. Particular emphasis will be placed on the relation to pion-nucleon scattering. This is relevant, since in the language of nuclear reaction theory, photopion production represents the "reaction channel" for the scattering. We shall also be interested in a comparison with specific models which have been proposed to describe pion-nucleon interactions.

In general terms, we should like to inquire to what extent we can find the elements of the S-matrix for photoproduction. These are the off-diagonal elements of the same S-matrix whose diagonal elements are determined by the phase shifts for pion scattering. The latter problem was first studied by Anderson, Fermi, Martin, and Nagle[1] and has since been pursued by many people. The present analysis concerns the corresponding problem for photopion production. An analysis along similar lines has been made by Hayakawa, Kawaguchi, and Minami.[2]

Just as was the case for the pion scattering, a model is necessary here for the detailed analysis. The model which we accept has been generally employed in the interpretation of pion phenomena at "low energies." (By "low energies" for photoproduction, we specifically mean γ-ray energies of less than 400 Mev in the laboratory system.) It has been discussed in detail by Gell-Mann and Watson[3] and has the principal features:

(1) Few states of orbital angular momentum are involved in pion-nucleon interactions.

(2) Isotopic spin is a useful quantum number.

(3) The state of the pion-nucleon system having orbital angular momentum $l=1$, angular momentum $J=\frac{3}{2}$, and isotopic spin $I=\frac{3}{2}$ is one of strong, attractive interaction. We shall refer to this as the "(3,3)" state. This feature of the model was proposed by Brueckner[4] and has been the subject of some controversy. We shall, however, accept this as providing a useful hypothesis for analysis of the experiments, which is essentially the point of view adopted by de Hoffmann, Alei, Metropolis, and Bethe[5] in their study of pion scattering. In favor of the Brueckner hypothesis of strong interaction in the (3,3) state is the marked simplicity of the photomeson cross sections when analyzed in terms of it.

The four elementary photopion cross sections which will be of interest to us are:

$$\begin{aligned}
&\gamma+p\rightarrow\pi^++n, && (\pi^+)\\
&\gamma+p\rightarrow\pi^0+p, && (\pi^0)\\
&\gamma+n\rightarrow\pi^-+p, && (\pi^-)\\
&\gamma+n\rightarrow\pi^0+n. && (n\pi^0)
\end{aligned}\tag{1-1}$$

We shall follow the notations of I[3] in representing physical quantities pertaining to one of these processes by the superscript $(+)$, (0), $(-)$, or $(n0)$. Since there is little experimental information concerning the $(n0)$ processes, we cannot use it in our analysis. We shall, however be able to *predict* the cross section for this process.

In Sec. 2 we shall summarize the available experimental data on photomeson production. The general theory based upon an enhancement of the (3,3) state and including all the S- and P-wave terms is developed in Sec. 8 where expressions for the photopion corrections are obtained in terms of the multipole amplitudes and

* This work was supported in part by the U. S. Atomic Energy Commission.

† Partial support was given by the National Science Foundation. Also, it is a pleasure to acknowledge the hospitality of the Los Alamos Scientific Laboratory, where this work was completed.

[1] Anderson, Fermi, Martin, and Nagle, Phys. Rev. **91**, 1955 (1953).

[2] Hayakawa, Kawaguchi, and Minami, Progr. Theoret Phys. (Japan) **12**, 355 (1954); M. Kawaguchi and S. Minami, Progr. Theoret Phys. (Japan), **12**, 789 (1954).

[3] M. Gell-Mann and K. Watson (referred to as I), Ann. Rev. Nuc. Sci. **4**, 219 (1954).

[4] K. Brueckner, Phys. Rev. **86**, 106 (1952).

[5] de Hoffmann, Alei, Metropolis, and Bethe, Phys. Rev. **95**, 1586 (1954).

TABLE I. Average coefficients adopted for the expansion of the photopion angular distribution in the form $A+B\cos\theta+C\cos^2\theta$. The superscripts refer to the charge. The quantities A^0 and C^0 are explained in the text. (Units are 10^{-30} cm^2/sterad.)

k	A^+	B^+	C^+	$A_{\exp}{}^0$	$C_{\exp}{}^0$	A^0	C^0
200	9.3±0.5	−1.8±1.0	−3.3±1.6	3.5±0.5	−3.3±2.0	3.0±0.4	−2.8±1.7
230	13.1±0.5	−3.0±0.9	−5.7±1.0	7.4±1.0	−6.8±2.0	6.6±0.9	−6.1±1.8
260	16.9±0.5	−4.3±1.0	−7.4±1.0	13.3±1.5	−11.6±4.0	12.2±1.4	−10.7±3.7
290	18.9±0.5	−3.8±1.2	−7.9±0.9	22.0±1.0	−17.6±4.0	20.7±0.9	−16.6±3.8
320	18.4±0.5	−1.1±0.9	−7.2±0.9	25.8±1.0	−22.0±4.0	24.6±1.0	−20.9±3.8
350	15.3±0.5	+1.1±0.6	−5.4±0.9	23.3±0.8	−20.8±3.0	22.4±0.8	−20.0±2.9
380	11.3±0.4	+2.5±0.6	−3.0±0.7	17.8±1.5	−15.0±2.5	17.2±0.5	−14.5±2.4
410	8.2±0.4	+3.2±0.8	−0.8±0.8	12.8±0.4	−10.0±1.5	12.4±0.4	−9.7±1.5
440	6.2±0.3	+3.5±0.7	+0.4±0.8	9.2±0.4	−6.8±1.4	9.0±0.4	−6.6±1.4
470	4.7±0.3	+3.7±0.6	+1.0±0.8	7.0±0.4	−5.0±1.3	6.8±0.4	−4.9±1.3

the scattering phase shifts. Particular cases of the equations developed in Sec. 8 are discussed in Sec. 3 where the behavior of photoproduction near threshold is considered, and in Sec. 4 where only production leading to the (3,3) state is considered. It is shown in Sec. 5 that fair agreement with experiment may be obtained by neglecting all those products of matrix elements which do not involve at least one term leading to the (3,3) state. Section 6 considers the energy dependence of the matrix elements, and in Sec. 7 the π^-/π^+ ratio is calculated and compared with the experimental values.

2. THE EXPERIMENTAL DATA

Experimental information on the various photomeson reactions (1-1) is available in the forms summarized in this section. For π^+ and π^0 production from hydrogen, the differential cross section at various angles is known as a function of photon energy. These data may be summarized by analyzing the differential cross section for either process in the form

$$\sigma(\theta)=A+B\cos\theta+C\cos^2\theta$$

and giving the values of the coefficients A, B, and C as a function of energy. To simplify comparison with the theory, we have tried to choose "average" experimental values of A, B, and C taking into account all of the more recent and accurate data. The average values adopted for A^+, B^+, C^+, A^0 and C^0 are given in Table I. For π^+ production, the coefficient A^+ follows the low-energy data of Bernardini and Goldwasser[6] up to about 230 Mev, and then the average of data obtained by two different methods at the California Institute of Technology, up to 470 Mev. These two methods employ a magnetic spectrometer[7] and a counter telescope[8] respectively, to detect the photopions. The coefficients B^+ and C^+ are essentially averages of the CalTech data.[7,8] The π^+ data of Jenkins, Luckey, Palfrey, and Wilson at Cornell[9] are in reasonable agreement with the coefficients A^+, B^+, and C^+ adopted here. For details about the points of agreement and disagreement between the various experiments, and for references to other experimental work, see references 7, 8, and 15.

The coefficients A^0 and C^0 adopted for π^0 production are taken from the data of Oakley and Walker[10] at high energy (above 290 Mev) and follows fairly well below this energy the data of Goldschmidt-Clermont, Osborn, and Scott[11] from the Massachusetts Institute of Technology. We refer to these two papers for references to other experiments and for a comparison with the other data which are available. Older π^0 experiments, which have not been given as much weight, are those of Silverman and Stearns,[12] and Walker, Oakley, and Tollestrup.[13]

The coefficient B^0 is not shown in Table I. It is small at all energies,[10,11] but will not be used to provide any very interesting information for the theory.

After the present analysis was made, other experimental results have become available. These include measurements of positive photoproduction at Illinois[14] and Berkeley[15]; and measurements of neutral pion production at Illinois.[16,17] The inclusion of these data would not materially change the results of the present analysis.

Since the charged and neutral pion data are to be analyzed together by a theory which ignores the difference in mass, a slight difficulty is encountered at low energy since the theory does not provide for the difference in thresholds of the π^+ and π^0 production. Since the energy dependence near thresholds has a form which is determined by general considerations such as the density of states, we have tried to change the experimental values $A_{\exp}{}^0$ and $C_{\exp}{}^0$ of Table I into the values A^0 and C^0 which would be found if the π^0 threshold were the same as that for π^+. Specifically, $A^0=A_{\exp}{}^0(\rho_+p_+{}^2)/(\rho_0p_0{}^2)$ and similarly for C^0. The quantity ρ will be

[6] G. Bernardini and E. L. Goldwasser, Phys. Rev. **95**, 857 (1954).
[7] Walker, Teasdale, Peterson, and Vette, Phys. Rev. **98**, 210 (1955).
[8] Tollestrup, Keck, and Worlock, Phys. Rev. **98**, 220 (1955).
[9] Jenkins, Luckey, Palfrey, and Wilson, Phys. Rev. **95**, 179 (1954).
[10] D. C. Oakley and R. L. Walker, Phys. Rev. **97**, 1283 (1955).
[11] Goldschmidt-Clermont, Osborne, and Scott, Phys. Rev. **97**, 188 (1955).
[12] A. Silverman and M. Stearns, Phys. Rev. **88**, 1225 (1952).
[13] Walker, Oakley, and Tollestrup, Phys. Rev. **97**, 1283 (1955).
[14] Leiss, Robinson, and Penner, Phys. Rev. **98**, 201 (1955).
[15] Gordon W. Repp, University of California Radiation Report UCRL-2953 (unpublished).
[16] F. E. Mills and L. J. Koester, Jr., Phys. Rev. **98**, 210 (1955).
[17] L. J. Koester, Jr. Phys. Rev. **98**, 211 (1955).

defined in Sec. 3 (see Eq. (3-5)). p_+ and p_0 are the momenta of the π^+ and π^0 respectively, in the center-of-momentum system, assuming each was produced by the same photon energy. The correction factor is certainly not right at high energies, above the maximum in the cross section, but it is large only near threshold. (It is 5 or 6 percent at 300 Mev.) The "corrected" values, A^0 and C^0, of Table I will be used throughout this paper.

The average experimental values of A^+, B^+, C^+, A^0, and C^0 shown in Table II have been taken from smooth curves, so the errors at neighboring points are correlated. The errors have been estimated from the accuracy of the individual experiments, and from the degree of consistency between different experiments, and are intended simply to indicate the estimated accuracy of the experimental coefficients as a function of energy.

The photoproduction of π^- mesons from neutrons is not directly measurable, of course, but information is obtained about this process by measuring the ratio of π^- and π^+ production from deuterium. We shall use the data of Sands, Teasdale, and Walker,[18] for this ratio, together with some recent unpublished data at 104° obtained by these same authors and Michel Bloch. These data are shown in Fig. 12 where they are compared with the theoretical calculations. References to earlier experimental work on the π^-/π^+ ratio are given in reference 18. Some measurements on the π^-/π^+ ratio have also been made at Illinois at low energies, but these are not yet published.[19]

Photoproduction of π^0 from neutrons is the least known of the reactions (1-1). Some data on the ratio of π^0 production from deuterium and hydrogen[20,21] are available, but the interpretation of these is less clear than that of the π^-/π^+ ratio from deuterium. The difficulty is that the π^0 production from the proton in deuterium may not be the same as that from the free proton in hydrogen. Experimentally, the ratio of π^0 production from deuterium and hydrogen per nucleon is about 0.9 with little energy dependence or angular dependence.

TABLE II. The multipole amplitudes for S- and P-wave photomeson production. The decomposition into isotopic-spin substates is made in the last column, using the notation of Anderson *et al.*[1] for the scattering phase shifts.

l	J	Amplitude of-pion wave	Multipolarity	Isotopic-spin substate	Amplitude
0	$\frac{1}{2}$	E_d	electric	$\frac{1}{2}$	E_1
			dipole	$\frac{3}{2}$	E_3
1	$\frac{1}{2}$	$M_d(\frac{1}{2})$	magnetic	$\frac{1}{2}$	M_{11}
			dipole	$\frac{3}{2}$	M_{31}
1	$\frac{3}{2}$	$M_d(\frac{3}{2})$	magnetic	$\frac{1}{2}$	M_{13}
			dipole	$\frac{3}{2}$	M_{33}
1	$\frac{3}{2}$	E_q	electric	$\frac{1}{2}$	E_{13}
			quadrupole	$\frac{3}{2}$	E_{33}

[18] Sands, Teasdale, and Walker, Phys. Rev. **95**, 592 (1954).

[19] Benventano, Bernardini, Lee, and Stoppini; quoted by Chew, reference 29, as obtaining the result: π^-/π^+ ratio $=1.5\pm0.1$ at 170 Mev.

[20] G. Cocconi and A. Silverman, Phys. Rev. **88**, 1230 (1952).

[21] Bingham, Keck, and Tollestrup, Phys. Rev. **98**, 1187 (A) (1955).

TABLE III. Scattering phase shifts used in this analysis.

k	α_{33}	α_1	α_3
200	5.9	7.5	−4.0
230	13.5	9.5	−7.5
260	24.8	9.2	−10.7
290	42.0	6.6	−14.0
320	66.5	3.0	−16.5
350	92.0	−1.5	−19.0
380	117	−6.0	−21.5
410	142	−10.0	−24.0

3. GENERAL FEATURES EXPECTED OF THE PHOTOPION CROSS SECTIONS

We shall assume that for the γ-ray energy in the laboratory system, $E_\gamma < 400$ Mev, the photopion cross sections are primarily determined by orbital S- and P-states of the final pion-nucleon system. Estimates have been made, however, of the effect of D-states and states of higher orbital angular momentum. The states contributing are summarized in Table II.

The amplitudes E_d, $M_d(\frac{3}{2})$, etc. are essentially the elements of the S-matrix for photoproduction, but they differ from these by multiplicative constants and a factor k. The multipole amplitudes E_d, etc. must be specified for each of the four elementary processes (1-1). Since we are using the relations obtained from charge independence, these may be expressed in terms of the amplitudes for isotopic-spin substates, which are listed in Sec. 8. Their derivation was indicated in I.[3] For our purposes, it is important to note that the quantities in the last column of Table II are real and that the relations between E_d and E_1, and E_3, etc., involve explicitly complex functions of the pion-nucleon phase shifts.[2,3,22] (See Sec. 8 and reference 3.)

For this reason, we must assume that the pion-nucleon scattering phase shifts are known. Those of de Hoffmann *et al.*[5] will be accepted for our analysis, since these are in agreement with the "(3,3) enhancement model" to be described in the next section. Admittedly, other sets of phase shifts are expected to be compatible with other models of photoproduction. On the other hand, we are aware of no other model which seems to indicate as much simplicity in the experimental cross sections as does the (3,3) model. The scattering phase shifts used are shown in Table III.

For only S- and P-wave pion emission, the photomeson cross section in the center-of-mass system takes the form discussed in Sec. 2:

$$\sigma(\theta)=A+B\cos\theta+C\cos^2\theta, \tag{3-1}$$

[22] K. Watson, Phys. Rev. **95**, 228 (1954).

where θ is the angle between the direction of motion of the γ ray and pion.

In terms of the amplitudes of Table II, the coefficients in Eq. (3-1) are[23]

$$A=|E_d|^2+|X|^2+|Y|^2,$$
$$C=|K|^2-|X|^2-|Y|^2, \tag{3-2}$$
$$B=-2\,\mathrm{Re}\{E_d{}^*K\},$$

where

$$X=\tfrac{3}{2}M_d(\tfrac{3}{2})+\tfrac{1}{4}E_q,$$
$$Y=\tfrac{1}{2}[M_d(\tfrac{3}{2})-\tfrac{1}{2}E_q]+M_d(\tfrac{1}{2}), \tag{3-3}$$
$$K=[M_d(\tfrac{3}{2})-\tfrac{1}{2}E_q]-M_d(\tfrac{1}{2}).$$

For γ-ray energies sufficiently near threshold that the scattering phase shifts are small (say for $E_\gamma<225$ Mev), the quantities X, Y, K, and E_d are real. In this case, the S- and P-wave contributions to the cross sections may be separated, using Eqs. (3-2) and the experimentally determined coefficients A, B, and C. We have

$$A+C=E_d^2+K^2$$

and

$$B=-2E_dK, \tag{3-4}$$

from which E_d and K may be found. X^2+Y^2 may next be determined from either A or C.

The analysis of the low-energy cross sections may be carried further if we make use of the energy dependence expected of reaction cross sections near threshold. We introduce the quantity[3]

$$\rho\equiv\frac{\eta}{\nu[1+\nu\mu/M][1+(\eta^2+1)^{\frac{1}{2}}\mu/M]}, \tag{3-5}$$

where μ is the pion rest mass and M is that for the nucleon. η and ν are the pion and photon momenta, respectively, in the center-of-mass (c.m.) system in units of (μc). Then[24]

$$E_d^2=\rho g_S,$$
$$X^2+Y^2=\eta^2\rho g_P,$$
$$C=-\eta^2\rho g_2,$$
$$B=-\eta\rho g_1, \tag{3-6}$$

where g_S, g_1, g_2, and g_P are constants near threshold (which probably refers to $E_\gamma<225$ Mev for π^+-photoproduction) and can each be directly determined from experiment. From Eqs. (3-2) and (3-6) we obtain[3]

$$g_1^2=4g_S[g_P-g_2]. \tag{3-7}$$

This represents a very general relation between the experimentally observable g's, which is valid if only S- and P-wave pion production occurs.

We may generalize relation (3-7) by including the S–D interference term, as follows. S–D wave interference adds to Eq. (3-1) the term

$$A_{SD}[\cos^2\theta-\tfrac{1}{3}], \tag{3-8}$$

where A_{SD} represents the strength of the S–D interference. This, of course, does not change the form of Eq. (3-1), but it modifies Eqs. (3-2) to

$$A=|E_d|^2+|X|^2+|Y|^2-\tfrac{1}{3}A_{SD},$$
$$C=|K|^2-|X|^2-|Y|^2+A_{SD},$$
$$B=-2\,\mathrm{Re}\,[E_d{}^*K]. \tag{3-9}$$

Near threshold, A_{SD} will have the form[24]

$$A_{SD}=\eta^2\rho g_{SD}, \tag{3-10}$$

where g_{SD} is a constant. The value of g_{SD} gives a direct indication of the importance of D-waves near threshold.

To proceed, we now expand our quantities in a power series of η,[25] (keeping all terms up to and including η^3):

$$A=\rho g_S+\eta^2\rho g_{03},$$
$$C=-\eta^2\rho g_{23},$$
$$B=-\eta\rho g_1,$$
$$E_d^2=\rho g_S+\eta^2\rho g_{S3}. \tag{3-11}$$

We now obtain from Eq. (3-9),

$$g_1^2=4g_S[g_{03}-g_{23}-(\tfrac{2}{3}g_{SD}+g_{S3})]. \tag{3-12}$$

Since g_1, g_{03}, g_S, and g_{23} are directly observable, Eq. (3-12) permits us to determine

$$\tfrac{2}{3}g_{SD}+g_{S3}.$$

Physically, this represents the net contribution to the cross section due to the *finite* size of the nucleon.

Experimental angular distributions are as yet rather incomplete for $E_\gamma<225$ Mev. Because of the smallness of g_S for the π^0 cross sections we can apply Eq. (3-12) to the π^+ cross sections only. From our subsequent study, it will appear that

$$g_{03}\simeq(8\pm1)\times10^{-30}\ \mathrm{cm}^2,$$

whereas $(\frac{2}{3}g_{SD}+g_{S3})$ is probably at most one-tenth of this. This indicates a small effect from nucleonic structure, as will become even more apparent from our subsequent analysis of the higher energy data.

It is quite interesting that pseudoscalar meson perturbation theory predicts

$$\tfrac{2}{3}g_{SD}=-g_{S3}$$

to the order in η to which our analysis applies. Thus, the observed smallness of $(\frac{2}{3}g_{SD}+g_{S3})$ results from a cancellation rather than from the smallness of D-wave terms.

[23] See, for instance, reference 3. The notation is due to Fermi (unpublished). The usefulness of this form for the cross sections appears at very low energies, as will be seen below. In Eqs. (3-2), the statistical weighting factor W of reference 3 has been absorbed into the quantities X, Y, K, and E_d, etc.

[24] The factor ν^{-1} in ρ is not determined from general considerations, but appears in π-meson field theory. This question will later be discussed in more detail. The ν-dependence of Eq. (3-10) is also not determined by any general principles.

[25] There is no point in expanding the factors in the denominator of ρ Eq. (3-5).

The foregoing has been described to emphasize that for energies low enough that the scattering phase shifts are small the cross sections are subject to a particularly simple, general analysis not possible at higher energies. A more detailed comparison with experiment was given in reference 3. The remainder of the present paper will be concerned with the "(3,3) enhancement model." This model appears to make it possible to analyze the cross sections into partial waves for threshold $<E_\gamma <400$ Mev. By its use of the isotopic spin, this model involves a simultaneous discussion of all *four* of the elementary cross sections (1-1).

4. THE "(3,3) ENHANCEMENT MODEL"

Roughly speaking, the (3,3) enhancement model supposes that those matrix elements leading into the final (3,3) state of the pion-nucleon system dominate the P-wave contributions to the photopion cross section. In terms of the matrix elements of Table II, this means that M_{33} and E_{33} are appreciably larger in magnitude than the other P-wave matrix elements.

We have, for instance, for the quantity X^+ of Eq. (3-3)[26]

$$X^+=e^{i\alpha_{33}}\frac{1}{\sqrt{2}}[3M_{33}+\tfrac{1}{2}E_{33}] + \frac{1}{2\sqrt{2}}[3(M_{13}-\delta M_{13})+\tfrac{1}{2}(E_{13}-\delta E_{13})]. \quad (4\text{-}1)$$

Similar expressions may be written for X^0 and the other quantities occurring in Eqs. (3-2), as is seen from Sec. 8.

The first bracket in X^+ (divided by $\sqrt{2}$) represents the contribution from the "enhanced" (3,3) state. The second bracket (divided by $2\sqrt{2}$) represents "nonenhanced" matrix elements. Calling the "enhanced" and "nonenhanced" matrix elements, M_e and M_n, respectively, we have

$$X^+=e^{i\alpha_{33}}M_e+M_n. \quad (4\text{-}2)$$

where M_e and M_n are real. Thus

$$|X^+|^2=M_e^2+2M_eM_n\cos\alpha_{33}+M_n^2. \quad (4\text{-}3)$$

A similar decomposition into "enhanced" and "nonenhanced" matrix elements can be made for Y and K for each of the four elementary cross sections (1-1).

We shall call the *simple enhancement model* that which results from neglecting all "nonenhanced" matrix elements (for example, we would set $M_n=0$ in Eqs. (4-2) and (4-3)).

The *general enhancement model* results from keeping only linear terms in the "nonenhanced" matrix elements in the cross sections. Thus, for example, in Eq. (4-3) we would neglect the M_n^2 term, having just

$$|X^+|^2\simeq M_e^2+2M_eM_n\cos\alpha_{33}. \quad (4\text{-}4)$$

The factor of $\cos\alpha_{33}$ which necessarily occurs is of importance for our subsequent analysis.

The justification for neglecting the terms such as M_n^2 depends on the magnitude of the *enhancement factor*, defined to be

$$\epsilon\equiv|M_e/M_n|. \quad (4\text{-}5)$$

As a result of our analysis the various enhancement factors, ϵ, can be determined experimentally. It will appear that in all cases, for $E_\gamma<350$ Mev, $\epsilon\geq 5$, which means that the neglected terms M_n^2 are less than 1/25 of the terms kept in equations such as (4-4). This demonstrates the consistency of the neglect of these quantities. The enhancement factor ϵ is of interest, since it provides a measure of the importance of the (3,3) state in determining the photomeson cross sections.

We shall begin our study by comparing the *simple enhancement model* with experiment.[27,28]

A. The Magnetic Dipole Model

Because of the relatively large anomalous magnetic moments of nucleons, one might guess that the magnetic dipole are more important than the electric quadrupole transitions.[27] This conclusion is qualitatively supported by meson field theory.[29] This suggests keeping only M_{33} of the P-wave multipole amplitudes, as a first approximation to the simple enhancement model. In this case, the coefficients of Eq. (3-1) have the form (for the π^+ and π^0 cross sections)

$$\begin{aligned} &A^+=A_S+A_P^+=A_S+(5/2)A_M,\\ &C^+=-\tfrac{3}{2}A_M,\\ &B^+=-\tfrac{2}{3}(A_SA_M)^{\frac{1}{2}}[\cos(\alpha_{33}-\alpha_3)+2\cos(\alpha_{33}-\alpha_1)], \quad (4\text{-}6)\\ &A^0=2A_P^+,\\ &C^0=2C^+. \end{aligned}$$

Here

$$A_S\equiv|E_d^+|^2, \quad (4.7)$$

which represents the S-wave contribution to $\sigma^+(\theta)$. In Eq. (4-6) we have neglected the S-wave contribution to $\sigma^0(\theta)$, since this is known to be small experimentally. We also define

$$A_P^+=A^+-A_S. \quad (4\text{-}8)$$

We shall use the quantities A_S and A_P^+, as defined by Eqs. (4-7) and (4-8), frequently throughout this paper. The quantity A_M is [see Eqs. (4-11) and (4-12)]

$$A_M=2[M_{33}]^2. \quad (4\text{-}9)$$

Equations (4-6) express the five experimentally known quantities A^+, $\cdots C^0$ in terms of only two parameters, A_S and A_M.

[26] We recall that the superscript "+" refers to the π^+ cross section of expressions (1-11). We also recall that we have agreed to set equal to zero, all P-wave scattering phase shifts except α_{33}.

[27] K. Brueckner and K. Watson, Phys. Rev. **86**, 923 (1952).
[28] B. Feld, Phys. Rev. **89**, 330 (1953).
[29] G. F. Chew, Phys. Rev. **95**, 1669 (1954).

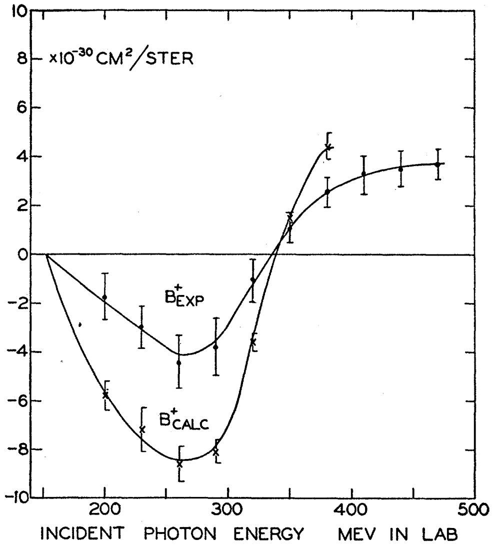

FIG. 1. The coefficients B^+ for π^+ production as calculated from the magnetic dipole model, Sec. 4A, compared to the experimental values.

The first difficulty with Eqs. (4-6) is that the value of B^+ is too large if A_S and A_M are chosen to give the observed values of A^+ and C^+. This may be seen from Eq. (3-7) if we use the condition from Eqs. (4-6) that $g_P=(5/3)g_2$. Taking from reference 3 the values for the g's [$g_1\simeq 3.0$, $g_2=3.5$, $g_S\simeq 10$, all in units of 10^{-30} cm²], we obtain a discrepancy of about a factor of 10 in the observed and calculated values of g_1^2 from Eq. (3-7). In Fig. 1, we compare the observed and calculated values of B^+. The calculated values are obtained from Eqs. (4-6), choosing A_S and A_M to give the experimentally observed A^+ and C^+. Equations (4-6) also imply that

$$A^0/C^0=5/3=1.67. \tag{4-10}$$

The experimental ratio is considerably smaller, being 1.22 ± 0.10 at all energies below 440 Mev,[10] although it is not known very accurately at the lower energies.

It seems apparent that we must conclude that this model is inadequate to explain the cross sections $\sigma^+(\theta)$ and $\sigma^0(\theta)$ even at moderately low energies. We, therefore, investigate the unrestricted *simple enhancement model*, for which electric quadrupole transitions are permitted.

B. The Simple Enhancement Model

We now drop all P-wave multipole amplitudes which do not lead to pion production in the (3,3) state, but keep an arbitrary admixture of magnetic dipole and electric quadrupole transitions to this state. We also neglect S-wave contributions to $\sigma^0(\theta)$.[30]

[30] A more thorough development is given in Sec. VIII, where Eqs. (4-11) and (4-12) are derived.

Then we have

$$\begin{aligned}
&A^+=A_S+A_P{}^+=A_S+A_{X0}+\tfrac{1}{4}A_{K0},\\
&C^+=\tfrac{3}{4}A_{K0}-A_{X0},\\
&B^+=-\tfrac{2}{3}(A_SA_{K0})^{\frac{1}{2}}[\cos(\alpha_{33}-\alpha_3)+2\cos(\alpha_{33}-\alpha_1)],\\
&A^0=2A_P{}^+,\quad C^0=2C^+.
\end{aligned} \tag{4-11}$$

Here A_{X0} and A_{K0} represent the "enhanced" P-wave contributions to the cross section, A_{K0} arises from P-waves which interfere with the S-wave and A_{X0} from those which do not interfere. Explicitly,[30]

$$\begin{aligned}
A_{K0}&=2[M_{33}-\tfrac{1}{2}E_{33}]^2,\\
A_{X0}&=\tfrac{1}{2}[3M_{33}+\tfrac{1}{2}E_{33}]^2.
\end{aligned} \tag{4-12}$$

It is evident from Eqs. (4-12) that knowledge of A_{K0} and A_{X0} permits us to determine individually the multipole amplitudes M_{33} and E_{33}. A_S again represents the S-wave contribution to $\sigma^+(\theta)$ and is given by Eq. (4-7). [If we set $E_{33}=0$ in Eqs. (4-12), Eqs. (4-11) reduce to the form of Eqs. (4-6).]

We have now three quantities, A_S, A_{X0}, and A_K to be determined. This may be done using $\sigma^+(\theta)$ only (i.e., A^+, C^+, and B^+). Having done this, we can use the last two equations of (4-11) to uniquely predict the coefficients A^0 and C^0 of $\sigma^0(\theta)$.

These calculated values are compared with the experimentally observed values in Fig. 2. The discrepancy between these values appears to be rather consistently larger than is expected from the assigned experimental errors.

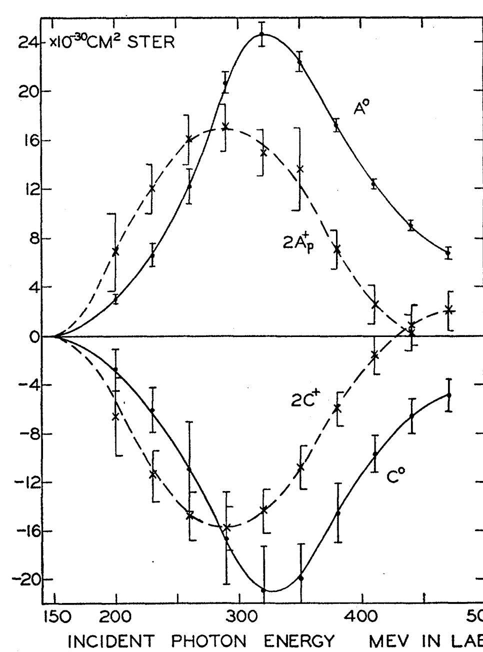

FIG. 2. Coefficients A^0 and C^0 for π^0 production as calculated from the π^+ data using the simple enhancement model, Sec. 4B are shown by the dashed curves and are labeled $2A^+$ and $2C^+$, respectively. The experimental values of A^0 and C^0 are shown for comparison.

It is thus our conclusion that the simple enhancement model fails to describe all of the observed detail in the cross sections. We consequently turn in the next section to the *general enhancement model* in the hope of obtaining a quantitative description of the experiments. We may remark here, however, that this study will imply that corrections to the simple enhancement model are rather small for $E_\gamma<400$ Mev and also that magnetic dipole contributions do appear to be appreciably more important than are electric quadrupole contributions for this range.

5. THE GENERAL ENHANCEMENT MODEL

We now keep first-order corrections to the cross sections arising from nonenhanced P-states. This means that we drop all squared matrix elements which are not enhanced, as in Eq. (4-4). The details are given in Sec. 8. The resulting π^+ and π^0 cross sections are finally

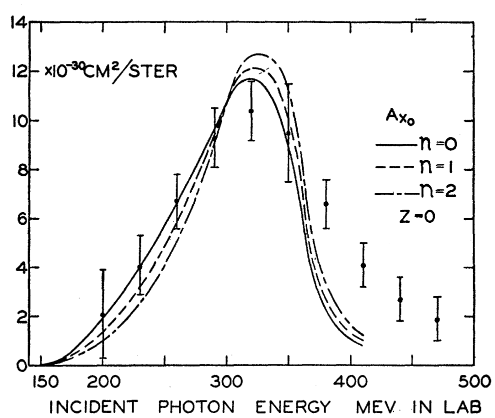

FIG. 3. "Experimental" values of A_{X0} from Table IV, compared to the theoretical energy dependence of Eqs. (6-3), for $Z=0$. The three curves are for $n=0$, $g_{X0}=7.5\times10^{-30}$ cm²/sterad; $n=1$, $g_{X0}=4.4\times10^{-30}$ cm²/sterad, and $n=2$, $g_{X0}=2.63\times10^{-30}$ cm²/sterad.

written in the form

$$
\begin{aligned}
A^+&=A_S+A_P{}^+\\
&=A_S+A_{X0}+\tfrac{1}{4}A_{K0}+A_{\Delta1}\cos\alpha_{33},\\
C^+&=\tfrac{3}{4}A_{K0}-A_{X0}-A_{\Delta1}\cos\alpha_{33},\\
B^+&=-\tfrac{2}{3}(A_SA_{K0})^{\frac{1}{2}}[\cos(\alpha_{33}-\alpha_3)+2\cos(\alpha_{33}-\alpha_1)],\\
A^0&=2A_P{}^+-3A_{\Delta1}\cos\alpha_{33},\\
C^0&=2C^++3A_{\Delta1}\cos\alpha_{33}.
\end{aligned}
\tag{5-1}
$$

The quantities A_S and $A_P{}^+$ have been defined by Eqs. (4-7) and (4-8). A_{X0} and A_{K0} have been defined by Eqs. (4-12). The new quantity appearing in Eqs. (5-1) is $A_{\Delta1}$, which represents the expected first order correction arising from nonenhanced P-waves. The factors of $\cos\alpha_{33}$ were anticipated in Eq. (4-4).

As is discussed in Sec. 8, Eqs. (5-1) represent an approximation to the general enhancement model. The exact model is developed there, as well as the experimental (and theoretical) justification for this approximation.

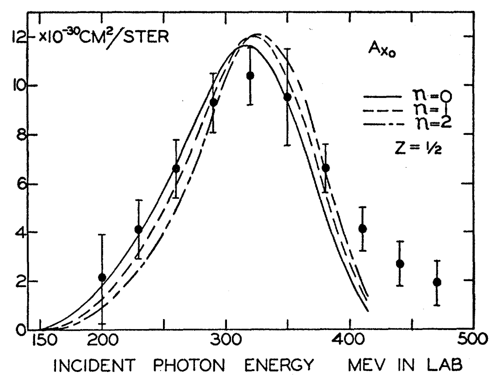

FIG. 4. Experimental values of A_{X0} compared to curves calculated from Eqs. (6-3) with $Z=\frac{1}{2}$. The three curves are for $n=0$, $g_{X0}=6.2\times10^{-30}$ cm²/sterad; $n=1$, $g_{X0}=3.6\times10^{-30}$ cm²/sterad, and $n=2$, $g_{X0}=2.03\times10^{-30}$ cm²/sterad.

There are four quantities to be determined at each energy from the experimental angular distributions. These are:

A_S—the σ^+ S-wave contribution;
A_{X0}—enhanced P-wave contribution, not interfering with S-waves;
A_{K0}—enhanced P-wave contribution, interfering with S-waves;
$A_{\Delta1}$—nonenhanced P-wave contribution, not interfering with S-waves.

$A_{\Delta1}$ is, of course, the product of two factors, one of which is enhanced and the other of which is not.

It is interesting that it is only the product $\cos\alpha_{33}A_{\Delta1}$ which is determined from the experiments. According to de Hoffmann and Bethe,[5,31] $\cos\alpha_{33}$ should pass through zero at $E_\gamma=345$ Mev. This means that the corrections to the simple enhancement model should change sign at about this energy—and in particular should be quite small in the energy region at which this occurs. We may

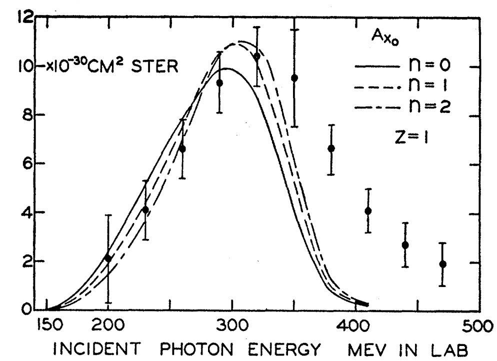

FIG. 5. Experimental values of A_{X0} compared to curves calculated from Eqs. (6-3) with $Z=1$. The three curves are for $n=0$, $g_{X0}=8.5\times10^{-30}$ cm²/sterad, $n=1$, $g_{X0}=5.6\times10^{-30}$ cm²/sterad; and $n=2$, $g_{X0}=3.38\times10^{-30}$ cm²/sterad.

[31] See Table III.

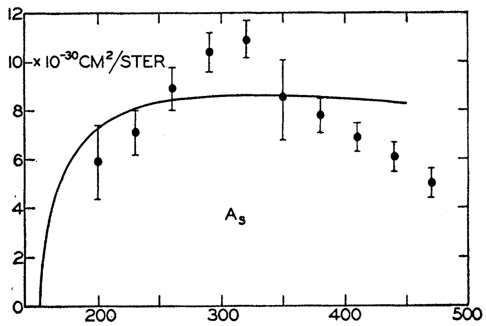

FIG. 6. "Experimental" values of A_S from Table IV, compared to the curve calculated from Eqs. (6-3) with $g_S=16.1\times10^{-30}$ cm²/sterad.

readily verify that the terms neglected in Eq. (5-1) are not sufficiently large to modify this conclusion (unless we keep higher partial waves than P-waves), if we accept the general characteristics of the (3,3) enhancement model.

To further study Eqs. (5-1), we observe that

$$A^{+}+C^{+}=A_S+A_{K0}. \tag{5-2}$$

This along with the equation for B^{+} permits us to determine A_S and A_{K0}. We may next use the equation

$$A_P{}^{+}=A^{+}-A_S$$

to determine

$$A_P{}^{+}=[A_{X0}+A_{\Delta 1}\cos\alpha_{33}]+\tfrac{1}{4}A_{K0}. \tag{5-3}$$

We are thus able to *explicitly separate* the S-wave and P-wave contributions to $\sigma^{+}(\theta)$, using just the *angular distribution* of $\sigma^{+}(\theta)$ at a given energy.

Having now $A_P{}^{+}$ and C^{+}, we may use either of the last two Eqs. (5-1) to determine $A_{\Delta 1}\cos\alpha_{33}$. As is indicated in Sec. 8, these two independent determinations are quite consistent with each other.

We now have determined each of the quantities in Eqs. (5-1). The values, as obtained from the experimental data summarized in Sec. 2, are tabulated in Table IV and are shown in Figs. 3–8.

The values of $A_{\Delta 1}\cos\alpha_{33}$, as given in Table IV, are shown in Fig. 8. The results seem to suggest that $\cos\alpha_{33}$ passes through zero at too low an energy. This is an

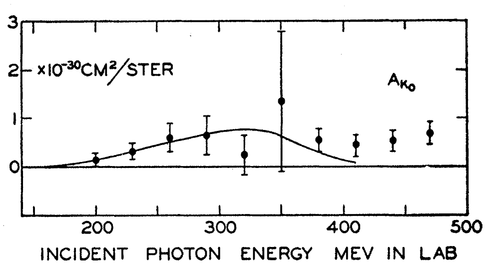

FIG. 7. "Experimental" values of A_{K0} from Table IV, compared to curves calculated from Eqs. (6-3) with $Z=\frac{1}{2}$, $n=0$, $g_{K0}=0.41\times10^{-30}$ cm² sterad.

extremely important point for the present model. It should be realized that the value of $A_{\Delta 1}\cos\alpha_{33}$ depends upon a comparison of the absolute cross sections $\sigma^{+}(\theta)$ and $\sigma^{0}(\theta)$. Insofar as the discrepancy seems to be real, one has two alternatives (other than giving up the (3,3) enhancement model) to explain this:

(1) The P-wave scattering phase shifts other than α_{33} are too large to equate to zero, as we have done. To explain the indicated discrepancy would require that some of these phase shifts be in excess of 30° for $E_\gamma\simeq300$ Mev, however, and that some fortuitous cancellation of matrix elements occur. Such large P-wave phase shifts (other than α_{33}) seems in disagreement with the de Hoffmann-Bethe determination. This explanation we consider rather unlikely.

(2) Higher partial waves may account for the discrepancy. Since the discrepancy apparently observed is associated with the finer details in the cross sections ($A_{\Delta 1}$ represents a moderately small contribution to the cross sections) this need not represent a very big effect.

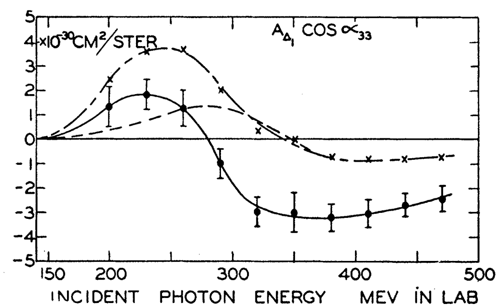

FIG. 8. $A_{\Delta 1}\cos\alpha_{33}$, showing the effect of including higher partial waves as calculated with meson perturbation theory. The lower points (circles) are those from Table IV from the analysis in terms of S and P waves only. The upper points (crosses) are corrected for the effects of higher partial waves as discussed in Sec. 5. The dashed curve has the energy dependence expected from Eqs. (6-3), and is calculated with $g_{\Delta 1}=1.42\times10^{-30}$ cm² sterad.

In order to estimate the effect of higher partial waves, the analysis of Sec. 8 was supplemented by including these waves as predicted by meson field theory in the perturbation limit. No new parameters need be introduced since the contribution of the higher partial waves is uniquely predicted in terms of the S-wave amplitude. The effect of these terms on the shape of the angular distribution at two different energies is shown in Fig. 9. The effect of higher partial waves upon the determination of $A_{\Delta 1}\cos\alpha_{33}$ may be seen in Fig. 8. When only S and P waves are included in the theory, any deviation in the ratio of the π^{+} and π^{0} cross sections from that predicted by the simple enhancement model (Sec. IV, b) must be absorbed in the term $A_{\Delta 1}\cos\alpha_{33}$ of Eq. (5-1). Thus any effects of the higher partial waves are included in the values of $A_{\Delta 1}\cos\alpha_{33}$ as calculated in Table IV and shown in the solid curve of Fig. 8. If the calculated effect of the higher partial waves is removed, then one obtains the curve through the crosses in Fig. 8 as the

TABLE IV. Values of the parameters obtained for the general enhancement model. The last columns list the values of $A_{\Delta 1}\cos\alpha_{33}$ as calculated by the two methods indicated in the text. (Units 10^{-30} cm²/sterad.)

k^+	A_S	A_{K0}	A_{P^+}	A_{X0}	$A_{\Delta 1}\cos\alpha_{33}$	$A_{\Delta 1}\cos\alpha_{33}$
200	5.9±1.5	0.14±0.15	3.4±1.6	2.1±1.8	1.3±1.1	1.3±1.2
230	7.1±0.9	0.33±0.20	6.0±1.0	4.1±1.2	1.8±0.7	1.8±0.9
260	8.9±0.9	0.61±0.29	8.0±1.0	6.6±1.2	1.3±0.8	1.4±1.3
290	10.4±0.8	0.65±0.41	8.5±0.9	9.3±1.2	−1.2±0.7	−0.3±1.3
320	10.9±0.8	0.24±0.40	7.5±0.9	10.4±1.2	−3.3±0.7	−2.2±1.4
350	8.5±1.6	1.38±1.50	6.8±1.7	9.5±2.0	−2.9±1.2	−3.1±1.2
380	7.8±0.7	0.55±0.26	3.5±0.8	6.6±1.0	−3.4±0.6	−2.8±0.9
410	6.9±0.6	0.44±0.22	1.3±0.8	+4.1±0.9	−3.3±0.6	−2.7±0.7
440	6.1±0.6	0.54±0.22	0.1±0.7	2.7±0.9	−2.9±0.9	−2.5±0.7
470	5.0±0.6	0.69±0.22	−0.3±0.7	1.9±0.9	−2.5±0.6	−2.3±0.7

correction term $A_{\Delta 1}\cos\alpha_{33}$ due to nonenhanced P-waves alone.

From the coefficients given in Table IV one may calculate the values of E_d^+, M_{33}, and E_{33} using Eq. (4-7) and (4-12). Values for these amplitudes are plotted in Fig. 10. In order to indicate the relative importance of the magnetic dipole, electric quadrupole, and other contributions to the cross sections, it is convenient to consider the total cross section, e.g.,

$$\sigma^+=4\pi(A^++\tfrac{1}{3}C^+)$$
$$=4\pi(E_d^{+2}+4M_{33}^2+\tfrac{1}{3}E_{33}^2+\tfrac{2}{3}A_{\Delta 1}\cos\alpha_{33}). \quad (5\text{-}5)$$

Since M_{33} and E_{33} are nearly equal, it is seen that M_{33} contributes about twelve times as much to the total cross section as E_{33}. This, as remarked above, might have been expected from theoretical calculations.

6. THE ENERGY DEPENDENCE OF THE MATRIX ELEMENTS

We have obtained in the last section the energy dependence of the various partial waves which contribute to $\sigma^+(\theta)$ and $\sigma^0(\theta)$. It is of interest to compare this with various predictions from theory of the expected energy dependence.

For energies near threshold, this has been discussed in Sec. 3. For higher energies, it has generally been thought that the enhanced multipole amplitudes should contain a factor[22,29] $\sin\alpha_{33}/\eta^3$.

Gell-Mann and Fermi[32] have suggested a generalization of this energy dependence. At a distance Z (in units of the pion Compton wavelength), the pion-nucleon scattering wave function for the (3,3) state contains the radial factor

$$\varphi=[j_1(\eta Z)\cos\alpha_{33}-n_1(\eta Z)\sin\alpha_{33}], \quad (6\text{-}1)$$

as long as Z is greater than the range of the scattering interaction. Here j_1 and n_1 are the regular and irregular spherical Bessel functions, respectively.[33] If we consider Z to be the "effective distance" from the nucleon at which photopions are produced, we may expect the photo cross section to be proportional to φ^2, the probability of finding a pion at a distance Z.[34] This then gives us a predicted energy dependence for the cross sections.

To be specific, we define

$$F(Z)=\frac{\varphi/\eta}{(\varphi/\eta)_{\eta=0}}; \quad (6\text{-}2)$$

so $F=1$ when $\eta=0$. We can combine this with the proper powers of η to give the correct threshold energy dependence. If we accept the S-wave energy dependence of Eq. (3-6) and an arbitrary power law for the ν dependence, we obtain

$$\begin{aligned}A_S&=\rho g_S,\\ A_{X0}&=\nu^n\eta^2\rho F^2 g_{X0},\\ A_{K0}&=\nu^n\eta^2\rho F^2 g_{K0},\\ A_{\Delta 1}&=\eta^2\rho F g_{\Delta 1},\end{aligned} \quad (6\text{-}3)$$

where n is an unknown number and ρ is given by Eq. (3-5). g_S, g_{X0}, g_{K0}, and $g_{\Delta 1}$ are constants. It is to be noted that only one factor of F is included in $A_{\Delta 1}$,

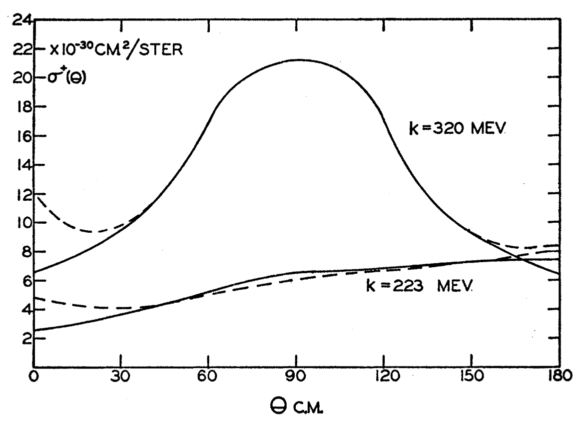

FIG. 9. The effect on the shape of the π^+ angular distribution of including higher partial waves as calculated with perturbation theory, (dashed curves). The solid curves include only S- and P-waves as in Eq. (5-1).

[32] M. Gell-Mann and E. Fermi (unpublished).

[33] L. I. Schiff, *Quantum Mechanics* (McGraw-Hill Book Company, Inc., New York, 1949).

[34] Such arguments have frequently been used in connection with pion phenomena. See, for instance, K. Watson, Phys. Rev. 88, 1163 (1952), for a more detailed justification of the arguments used.

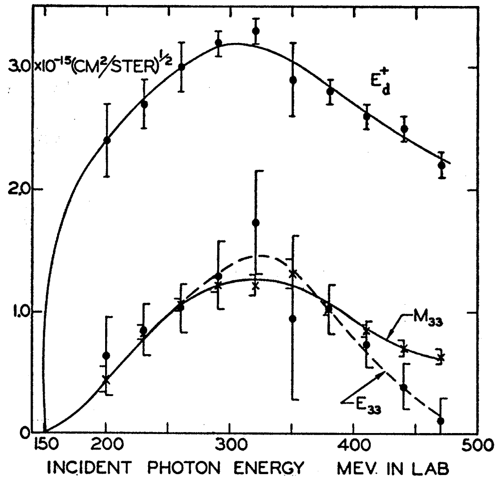

FIG. 10. The quantities E^+, M_{33}, and E_{33} as a function of energy, as determined by analysis of the π^+ and π^0 data using the general enhancement model, Sec. 5.

since it contains only one factor which is enhanced. The form given for $A_{\Delta 1}$ implies that the nonenhanced amplitudes increase with η. For $E_\gamma < 400$ Mev this seems, at least roughly, to be the case.

For $\eta Z \ll 1$,

$$F(0) = \frac{\sin\alpha_{33}/\eta^3}{(\sin\alpha_{33}/\eta^3)_{\eta=0}}, \tag{6-4}$$

in agreement with previous[22,29] estimates of the energy dependence. For $E_\gamma < 400$ Mev, we have $\eta < 2.2$, which means that nucleonic structure effects are not expected to show up in our analysis if they are confined to $Z < \frac{1}{2}$. We do not, of course, mean to take the expressions (6-1) and (6-2) very literally as telling us at just "what distance" mesons are produced. However, it is reasonable to expect $F(0)$, as given by Eq. (6-4) to give a quantitative prediction when ηZ is small and also for Eq. (6-2) to describe qualitatively the energy at which structure effects may appear. In any case, structure effects do not seem very important for $E_\gamma < 400$ Mev.

The dependence of the terms in Eq. (6-3) on the photon momentum ν is of course not known from general principles. The form given for A_S is that predicted by meson theory and seems to fit the data very well for $E_\gamma < 400$ Mev. It might be felt that some such factor as $[(1/\nu)j_1(\nu Z)]^2$ should be included in A_{X0} and A_{K0}. In view of the fact that Z seems to be too small to be of much importance, this factor is assumed to be constant and absorbed in the constants g_{X0} and g_{K0}.

In Figs. 3, 4, and 5, we compare A_{X0} as calculated from Eqs. (6-3) with the observed values (Table IV) for $n=0$, 1, 2 and for $Z=0$, $\frac{1}{2}$, and 1. The value of g_{X0} was adjusted in each case to give a best fit. It is probably not possible to pick the "best" value of n from these curves. Fortunately, the curves for different Z are not very different, although $Z=1$ seems clearly too large. We shall arbitrarily take $n=0$ for our subsequent arguments, pending future considerations which might make another value preferable. $n=0$ is, incidentally, predicted by meson field theory in the perturbation limit. We shall also take $Z=\frac{1}{2}$, although a "best" value of Z is probably somewhat smaller, perhaps 0.3 or 0.4.

A least squares determination of the g's of Eqs. (6-3) has been made (with $n=0$, $Z=\frac{1}{2}$, as specified above). The values are listed in Table V.

To illustrate this we use these four constants from Table V and Eqs. (6-3) to calculate the photopion cross sections [Eqs. (5-1)]. These calculations are compared with experiment in Figs. 11 and 12. The agreement is fairly good, with the exception of the coefficients A^+ and C^+ in the region of the peak at $E_\gamma \simeq 320$ Mev, and A^0 and C^0 above the peak, $E_\gamma > 350$ Mev. These discrepancies result in part from the fact that the energy dependence given by Eqs. (6-2) and (6-3) for the enhanced P-wave contributions seems to fall too rapidly at high energies. (See Figs. 3, 4, and 5.) Perhaps more important, however, is the discrepancy in the energy dependence of $A_{\Delta 1}\cos\alpha_{33}$ shown in Fig. 8. The possibility that this is associated with the contribution from D-waves was discussed in the previous section.

We must finally emphasize that our analysis is in any case not expected to be reliable above $E_\gamma = 400$ Mev, as is seen from Table IV. That is, above this energy $A_{\Delta 1}$ and A_{X0} become comparable which violates the assumption that the (3,3) P-waves are predominant.

7. THE π^-/π^+ RATIO

The most useful information concerning the cross section σ^- comes from the study of the π^-/π^+ ratio of photopions produced from deuterons. This, unfortunately, of course, does not give us the ratio from *free* nucleons because of (1) deuteron binding effects, and, (2), the possibility that the pion may be scattered by the two nucleons before getting out of the range of their interaction. A satisfactory discussion of these effects has not been made, to our knowledge.

To a first approximation we may argue, however, that binding and scattering effects tend to cancel for the π^-/π^+ ratio from deuterium, permitting us to interpret this as being roughly the same as for free nucleons. The arguments for this were given in reference 22, the point being that for energies high enough that Coulomb effects could be neglected the *charge-inde-*

TABLE V. Values of the constants g_S, g_X, etc. which appear in Eqs. (6-3), (7-3), (7-2), and (11-12).[a] Units for all but r are 10^{-30} cm²/sterad.

$g_S = 16.1 \pm 0.6$,	$r = 0.113 \pm 0.005$,
$g_{X0} = 6.15 \pm 0.38$	$g_{\delta k} = 0.48 \pm 0.03$,
$g_{K0} = 0.41 \pm 0.11$,	$g_{\delta 1} = 0.47 \pm 0.24$,
$g_{\Delta 1} = 1.42 \pm 0.37$,	$g_{\Delta 3} = -0.04 \pm 0.38$,
$g_{K1} - 2g_{\Delta 3} = 0.12 \pm 0.21$,	$g_{K1} = 0.04 \pm 0.79$,
$g_p{}^+ = g_{X0} + \frac{1}{4}g_{K0} + g_{\Delta 1} = 7.7 \pm 0.5$.	

[a] Bernardini and Goldwasser (reference 5) obtain the values: $g_S = 15.1 \pm 1$ and $g_P{}^+ = 11 \pm 3$.

pendent nuclear binding effects in deuterium tend to modify the free nucleon cross sections π^- and π^+ in the same proportion. Thus, for the ratio σ^-/σ^+ the binding effects tend to cancel, giving very nearly the same value for deuterium as for free neutrons and protons. The discussion was given only for S-wave photopion production in reference 22. The extension to the practical case for which several multipole amplitudes contribute to photopion production can easily be made if we assume that the proportional modification due to deuteron binding effects is the same for each multipole amplitude.

Lacking, then, a more complete analysis, we shall assume that the ratio $\sigma^-(\theta)/\sigma^+(\theta)$ as measured for deuterium is the same as for free nucleons.

The difference between the cross sections $\sigma^-(\theta)$ and $\sigma^+(\theta)$ is due to the "nucleon recoil" terms of the multipole amplitudes is derived in Sec. 8. This is

$$\begin{aligned}\sigma^-(\theta)=\sigma^+(\theta)&+r(r+2)A_S\\&+\cos\alpha_{33}[A_{\delta 1}\sin^2\theta+A_{\delta K}\cos^2\theta]\\&+\cos\theta[rB^+-(1+r)(A_S/A_{K0})^{\frac{1}{2}}A_{\delta K}].\end{aligned}\quad(7\text{-}1)$$

Here A_S, B^+, and A_{K0} are the same quantities which occurred in Eqs. (5-1); r is a constant expressed in terms of the π^-/π^+ ratio at energetic threshold:

$$[\sigma^-(\theta)/\sigma^+(\theta)]_{\text{threshold}}=(1+r)^2. \quad (7\text{-}2)$$

$A_{\delta 1}$ and $A_{\delta K}$ are two new quantities having the form

$$A_{\delta 1}=\eta^2\rho F g_{\delta 1},\quad A_{\delta K}=\eta^2\rho F g_{\delta K}, \quad (7\text{-}3)$$

where $g_{\delta 1}$ and $G_{\delta K}$ are constants. We have assumed that the conclusions which we reached in Sec. 6 concerning the energy dependence of the multipole amplitudes are valid here also.

We have now three new constants, r, $g_{\delta 1}$, and $g_{\delta K}$ to be determined from the observed π^-/π^+ ratio. Since $g_{\delta 1}$ and $g_{\delta K}$ depend upon the nonenhanced P-waves, we expect them to be small compared with g_{X0} (to satisfy the condition of the general enhancement model that the largest P-wave amplitudes are those which lead to the final (3,3) state). Values for $g_{\delta 1}$, $g_{\delta K}$ and r have been determined from the experiments of Sands, Teasdale, and Walker,[18] together with some more recent data at 104° mentioned in Sec. 2. The values obtained are given in Table V. The smallness of $g_{\delta 1}$ and $g_{\delta K}$ is quite satisfactory from the point of view of the enhancement model. The value of r leads to

$$(\sigma^-/\sigma^+)_{\text{threshold}}=1.24, \quad (7\text{-}4)$$

which may be compared with the prediction from meson field theory that this be $(1+\mu/M)^2\simeq 1.3$.

Using the constants of Table V and Eqs. (5-1) and (7-1), we may calculate the ratio $\sigma^-(\theta)/\sigma^+(\theta)$. The calculated values are compared with the measured values in Fig. 13.

We may finally calculate a predicted cross section $\sigma(\theta)^{(n0)}$ using Eqs. (8-11). $A^{(n0)}=A^0-A_{\delta 1}\cos\alpha_{33}$. This

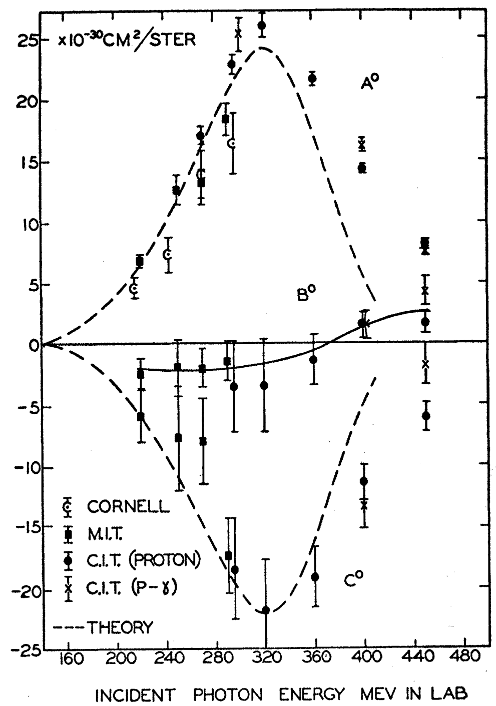

FIG. 12. Experimental values of A^0, B^0 and C^0 for π^0 production, compared to dashed curves for A^0 and C^0 calculated from Eqs. (5-1) and (6-3) with $Z=\frac{1}{2}$, $n=0$, and values of g_{X0}, etc. from Table V. The experimental data are taken from references 10, 11, 12 and 13. The M.I.T. points (reference 11) at 320 Mev disagree badly with the other data (probably because of difficulties in obtaining data so near the upper end of a bremsstrahlung spectrum), and have not been included in this figure.

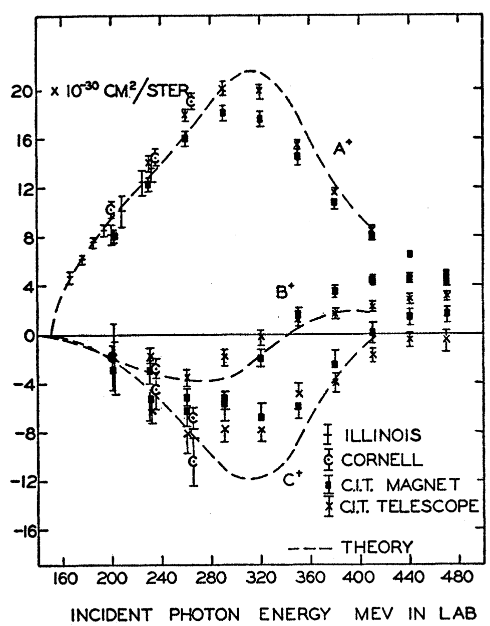

FIG. 11. Experimental values of A^+, B^+, and C^+ for π^+ production, compared to dashed curves calculated from Eqs. (5-1) and (6-3) with $Z=\frac{1}{2}$, $n=0$, and values of g_{X0}, etc. from Table V. The experimental data are taken from references 6, 7, 8 and 9.

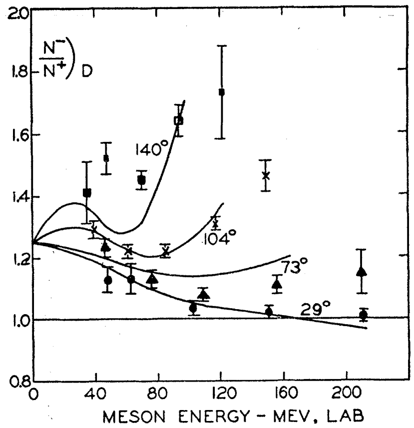

FIG. 13. The experimental π^-/π^+ ratio in deuterium compared to curves calculated by using Eqs. (5-1), (7-1), and the values of constants given by Table V.

differs from A^0 by a negligible amount except at the highest energies, and even at 410 Mev, the difference is only four percent.

Also $C^{(n0)}=C^0-\cos\alpha_{33}[A_{\delta K}-A_{\delta 1}]\simeq C^0$. $B^{(n0)}$ like B^0 is small. Thus, within a few percent, $\sigma^{(n0)}(\theta)=\sigma^0(\theta)$ and this is probably in sufficiently good agreement with the experiments,[20,21] considering the difficulties in interpretation of these, as mentioned in Sec. 2.

8. EXPRESSION OF CROSS SECTIONS IN TERMS OF MULTIPOLE AMPLITUDES

The photopion cross sections, when only S- and P-waves are important, are directly expressed in terms of the multipole amplitudes using Eqs. (3-1), (3-2), and (3-3). The next step of expressing these in terms of the amplitudes for final states of pure isotopic spin is given in references 3 and 22.

For convenience we summarize here the equations from reference 3 which express the amplitudes E_d, $M_d(\frac{3}{2})$, etc. for each of the four cross sections (1-1) in terms of the amplitudes for pure isotopic-spin states (see Table II).

$$
\begin{aligned}
E_d^+&=e^{i\alpha_3}\sqrt{2}E_3+e^{i\alpha_1}(1/\sqrt{2})[E_1-\delta E_1],\\
E_d^0&=e^{i\alpha_3}2E_3-e^{i\alpha_1}\tfrac{1}{2}[E_1-\delta E_1],\\
M_d^+(\tfrac{1}{2})&=e^{i\alpha_{31}}\sqrt{2}M_{31}+e^{i\alpha_{11}}(1/\sqrt{2})[M_{11}-\delta M_{11}],\\
M_d^0(\tfrac{1}{2})&=e^{i\alpha_{31}}2M_{31}-e^{i\alpha_{11}}[M_{11}-\delta M_{13}],\\
M_d^+(\tfrac{3}{2})&=e^{i\alpha_{33}}\sqrt{2}M_{33}+e^{i\alpha_{13}}(1/\sqrt{2})[M_{13}-\delta M_{13}],\\
M_d^0(\tfrac{3}{2})&=e^{i\alpha_{33}}2M_{33}-e^{i\alpha_{13}}\tfrac{1}{2}[M_{13}-\delta M_{13}],\\
E_q^+&=e^{i\alpha_{33}}\sqrt{2}E_{33}+e^{i\alpha_{13}}(1/\sqrt{2})[E_{13}-\delta E_{13}],\\
E_q^0&=e^{i\alpha_{33}}2E_{33}-e^{i\alpha_{13}}\tfrac{1}{2}[E_{13}-\delta E_{13}].
\end{aligned}
\tag{8-1}
$$

To obtain the corresponding quantities for the (π^-) from the (π^+) process and the $(n\pi^0)$ from the (π^0) process, we change the sign of δE_1, δM_{11}, δM_{13}, and δE_{13} in Eqs. (8-1).

The purpose of the present section is to reduce these general expressions to a convenient form for the analysis of the data within the framework of the (3,3) model.

A. S-waves

If we consider energies sufficiently near threshold that only S-wave pion production is important, the analysis is very simple.

In terms of the three S-wave amplitudes E_3, E_1, and δE_1, we define

$$
\begin{aligned}
E_0&=\sqrt{2}E_3+(1/\sqrt{2})[E_1-\delta E_1],\\
r&=\sqrt{2}\delta E_1/E_0,\\
r_0&=(1/E_0)\{2E_3-\tfrac{1}{2}E_1+\delta E_1\}.
\end{aligned}
\tag{8-2}
$$

When the S-wave phase shifts are small (as they actually are, according to de Hoffmann *et al.*[5]),

$$E_d^+=E_0. \tag{8-3}$$

The four differential cross sections are now (we are now neglecting P-waves!)

$$\sigma^+(\theta)=E_0^2;\quad \sigma^-(\theta)/\sigma^+(\theta)=(1+r)^2,$$
$$\sigma^{(n0)}(\theta)=r_0^2\sigma^+(0)$$

and

$$\sigma^0(0)=\tfrac{1}{2}(r+r_0\sqrt{2})^2\sigma^+(\theta). \tag{8-4}$$

Even when we do not neglect the S-wave phase shifts, we shall continue to use the definitions (8-2) as *given*.

B. The General Enhancement Model

We shall next write out the general form for the differential cross sections in the approximation of Eq. (4-4), keeping both S- and P-wave contributions. That is in the cross sections we shall drop the squares of all amplitudes which do not lead into the (3,3) state.

We first define

$$X_0=(1/\sqrt{2})[3M_{33}+\tfrac{1}{2}E_{33}],\quad K_0=\sqrt{2}[M_{33}-\tfrac{1}{2}E_{33}]. \tag{8-5}$$

From Eqs. (4-12), we see that

$$A_{X0}=X_0^2,\quad A_{K0}=K_0^2. \tag{8-6}$$

We further define

$$
\begin{aligned}
A_{\Delta 3}&=\sqrt{2}K_0M_{31},\\
A_{\Delta 1}&=(1/\sqrt{2})X_0\{3[M_{13}-\delta M_{13}]+\tfrac{1}{2}[E_{13}-\delta E_{13}]\}\\
&\quad+(1/2\sqrt{2})K_0\{[M_{13}-\delta M_{13}]-\tfrac{1}{2}[E_{13}-\delta E_{13}]\\
&\qquad+2[M_{11}-\delta M_{11}]\},\\
A_{K1}&=\sqrt{2}K_0\{[M_{13}-\delta M_{13}]-\tfrac{1}{2}[E_{13}-\delta E_{13}]\\
&\qquad-[M_{11}-\delta M_{11}]\}.
\end{aligned}
\tag{8-7}
$$

It should be recalled that in Sec. 5, we found the $X_0^2\gg K_0^2$. Comparison with Eqs. (8-7) suggests that $A_{\Delta 1}$ should then be larger than $A_{\Delta 3}$ or A_{K1}.

Since we have agreed to neglect all P-wave phase shifts, except for α_{33}, it is only a matter of algebraic manipulation to express the cross sections in terms of the quantities of Eqs. (8-6) and (8-7). We have (neglecting some obviously very small terms involving the S-wave phase shifts):

$$
\begin{aligned}
A^+ &= A_S + A_{X0} + \tfrac{1}{4}A_{K0} + \cos\alpha_{33}[A_{\Delta 1} + A_{\Delta 3}] \\
&= A_S + A_{P^+}, \\
C^+ &= \tfrac{3}{4}A_{K0} - A_{X0} + \cos\alpha_{33}[A_{K1} - A_{\Delta 1} - 3A_{\Delta 3}], \\
B^+ &= -\tfrac{2}{3}(A_S A_{K0})^{\frac{1}{2}}\{[\cos(\alpha_{33}-\alpha_3) + 2\cos(\alpha_{33}-\alpha_1)] \\
&\quad + \tfrac{3}{2}[1/A_{K0}][A_{K1} - 2A_{\Delta 3}] + (r+\sqrt{2}r_0) \\
&\quad \times[\cos(\alpha_{33}-\alpha_3) - \cos(\alpha_{33}-\alpha_1)]\}, \\
A^0 &= 2A_{P^+} - \cos\alpha_{33}[3A_{\Delta 1}], \\
C^0 &= 2C^+ + 3\cos\alpha_{33}[A_{\Delta 1} - A_{K1}], \\
B^0 &= -(4/3)(A_S A_{K0})^{\frac{1}{2}}\{[\cos(\alpha_{33}-\alpha_3) - \cos(\alpha_{33}-\alpha_1)] \\
&\quad + (r+\sqrt{2}r_0)[\cos(\alpha_{33}-\alpha_3) + \tfrac{1}{2}\cos(\alpha_{33}-\alpha_1)] \\
&\quad - (r+\sqrt{2}r_0)(3/8A_{K0})[A_{K1} + 4A_{\Delta 3}]\}. \qquad (8\text{-}8)
\end{aligned}
$$

We first discard the coefficient B^0 since it is not yet known sufficiently well experimentally to be useful. We also neglect the last term in B^+, since this is certainly very small.

The second term in brackets in B^+,

$$(3/2)\frac{1}{A_{K0}}[A_{K1} - 2A_{\Delta 3}],$$

must be small since it doesn't seem to effect the point at which B^+ passes through zero (see Sec. 5). Indeed, we can put limits on this term from the experimental data at that energy for which

$$\cos(\alpha_{33}-\alpha_3) + 2\cos(\alpha_{33}-\alpha_1) = 0.$$

Using the fact that we were able to determine the energy dependence of the multipole amplitudes, we can approximate the value of

$$A_{K1} - 2A_{\Delta 3} = (g_{K1} - 2g_{\Delta 3})\rho\eta^2 F$$

over our entire energy range by estimating the value of $g_{K1} - 2g_{\Delta 3}$ from the behavior of B^+. The result is

$$
\begin{aligned}
g_{K1} - 2g_{\Delta 3} &= \tfrac{2}{3}F g_{K0}(0.4 \pm 0.7 \times 10^{-30}) \\
&= 0.12 \pm 0.21 \times 10^{-30}\ \text{cm}^2/\text{sterad.}
\end{aligned}
$$

It seems clear from this that

$$A_{K1} \simeq 2A_{\Delta 3}, \qquad (8\text{-}9)$$

which permits us to eliminate A_{K1} from Eqs. (8-8). Using the five experimental coefficients, we can now determine all the quantities A_{X0}, A_{K0}, $A_{\Delta 1}$, $A_{\Delta 3}$, and A_S, as summarized in Table V. It is apparent that A_{K1} and $A_{\Delta 3}$ can both be neglected, as was to have been expected on theoretical grounds from the discussion following Eqs. (8-7).

Neglecting A_{K1} and $A_{\Delta 3}$, Eqs. (8-8) reduce immediately to Eqs. (5-1).

Before passing on, we note that in view of the smallness of A_{K0}, it is somewhat surprising that the term $(\frac{3}{2}/A_{K0})(A_{K1} - 2A_{\Delta 3})$ doesn't dominate the coefficient B^+. The mere fact that it doesn't seems to imply that Eq. (8-9) must be a good approximation.

To obtain the remaining two cross sections, we define

$$
\begin{aligned}
A_{\delta 1} &= -\sqrt{2}X_0(-3\delta M_{13} - \tfrac{1}{2}\delta E_{13}) \\
&\quad - (1/\sqrt{2})K_0(-\delta M_{13} + \tfrac{1}{2}\delta E_{13} - 2\delta M_{11}), \\
A_{\delta K} &= -2\sqrt{2}K_0(-\delta M_{13} + \tfrac{1}{2}\delta E_{13} + \delta M_{11}). \qquad (8\text{-}10)
\end{aligned}
$$

The (π^-) and $(n\pi^0)$ cross sections then have the form:

$$
\begin{aligned}
A^- &= (1+r)^2 A_S + A_{P^+} + \cos\alpha_{33}A_{\delta 1}, \\
C^- &= C^+ + \cos\alpha_{33}(A_{\delta K} - A_{\delta 1}), \qquad (8\text{-}11) \\
B^- &= (1+r)B^+ - (1+r)(A_S/A_{K0})^{\frac{1}{2}}A_{\delta K};
\end{aligned}
$$

and

$$
\begin{aligned}
A^{(n0)} &= A^0 - \cos\alpha_{33}A_{\delta 1}, \\
C^{(n0)} &= C^0 - \cos\alpha_{33}(A_{\delta K} - A_{\delta 1}), \\
B^{(n0)} &= -(4/3)(A_S A_{K0})^{\frac{1}{2}}\{(1+r)[\cos(\alpha_{33}-\alpha_3) \\
&\quad - \cos(\alpha_{33}-\alpha_1)] + \sqrt{2}r_0[\cos(\alpha_{33}-\alpha_3) \\
&\quad + \tfrac{1}{2}\cos(\alpha_{33}-\alpha_1)] - (1/4A_{K0})(3/\sqrt{2})r_0 \\
&\quad \times[A_{K1} + 4A_{\Delta 3} + A_{\delta K}]\}. \qquad (8\text{-}12)
\end{aligned}
$$

Equation (8-11) were used in Eq. (7-1).

In accordance with the determination of the energy dependence of the amplitudes, as was done in Sec. 6, we now define

$$A_{\Delta 3} = \eta^2\rho F g_{\Delta 3}, \quad A_{K1} = \eta^2\rho F g_{K1}. \qquad (8\text{-}13)$$

In Table V are listed the seven coefficients g_{X0}, g_{K0}, g_S, $g_{\Delta 1}$, $g_{\Delta 3}$, g_{K1}, $g_{\delta 1}$, and $g_{\delta K}$, as determined from the experiments as well as the constant r of Eq. (7-2).

9. CONCLUSIONS

Our analysis has consisted of two major subdivisions. The first has asked only that we be able to find S-matrix elements which are compatible with both the experimental data and with the (3,3) enhancement model. It appears that this can be done for $E_\gamma < 400$ Mev, but not for higher energies. A difficulty was probably encountered for $E_\gamma \simeq 300$ to 350 Mev (in the value of $A_{\Delta 1}\cos\alpha_{33}$), but can possibly be resolved by the inclusion of D-waves as predicted by meson field theory. This question involves a relatively small effect in the observed cross sections, however, so must likely await more experimental accuracy (say at $\theta = 90°$) in this energy range.

The second portion of our analysis has involved a comparison of the experimental S-matrix elements with those obtained from models. It was found, for instance, that the energy dependence is reasonably well determined by very elementary models for $E_\gamma < 350$ Mev. It has been suggested by Sachs[35] that the slight peak in A_S at $E_\gamma \simeq 300$ Mev might be due to an S-wave "resonance" of the pion-nucleon system (assuming that this peak has experimental significance).

[35] R. G. Sachs (private communication).

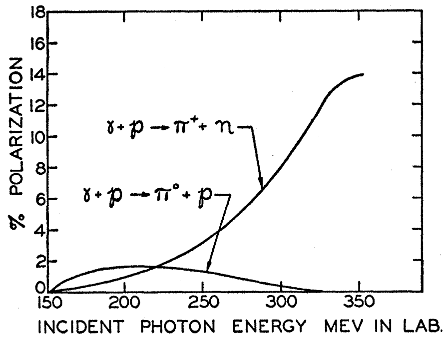

FIG. 14. The polarization of the recoil nucleon, as calculated from Eqs. (9-4).

None of the models has been very good in the 350–400 Mev energy range. This is not surprising, first, because our models have been *low*-energy models using arguments appropriate near energetic threshold, and, second because higher partial waves may become important in this energy region.

We observe that the (3,3) enhancement model has given a very natural and simple explanation for the gross features of the experiments. The detailed features show considerable complication, however.

A detailed test of the (3,3) enhancement model is, in principle, possible if the polarization of the recoil nucleon were to be measured.

If we define "spin up" in the direction $(\mathbf{k}\times\mathbf{q})$, where $\mathbf{k}$ and $\mathbf{q}$ are respective momenta of the γ ray and pion in the c.m. system, the polarization of the recoil nucleon is

$$P=\frac{\sigma(\uparrow)-\sigma(\downarrow)}{\sigma(\uparrow)+\sigma(\downarrow)}, \tag{9-1}$$

where $\sigma(\uparrow)$ and $\sigma(\downarrow)$ are the respective differential cross sections for photopion production when the final nucleon spin is "up" and "down."

We easily obtain

$$P=\frac{\sin\theta}{\sigma(\theta)}\{\mathrm{Im}[E_d^*(2M_d(\tfrac{1}{2})+M_d(\tfrac{3}{2})-\tfrac{1}{2}Eq)] \\ +3\,\mathrm{Im}[M_d^*(\tfrac{1}{2})(M_d(\tfrac{3}{2})-\tfrac{1}{2}E_q)]\cos\theta\}. \tag{9-2}$$

Here $\sigma(\theta)$ is the differential cross section (3-1) and "Im $(\cdots)$" means the "imaginary part of $(\cdots)$."

Experimental observation of the polarization could give quite useful additional information concerning the multipole amplitudes. For our purposes, the most interesting conclusions would be that direct information would be obtained concerning the validity of the (3,3) enhancement model. The reason for this is that the enhanced terms occur only in the combination

$$M_d(\tfrac{3}{2})-\tfrac{1}{2}E_q \tag{9-3}$$

in Eq. (9-2). This is the combination occurring in A_{K0}, which we have seen to be quite small (due to the tendency for the magnetic dipole and electric quadrupole terms to approximately cancel in Eq. (9-3). This means that the predicted polarization should be quite small on the basis of the (3,3) model. (For other models, with different "large" multipole amplitudes, this would not generally be the case.) Thus an observed large polarization would appear to be incompatible with (3,3) model.

Keeping only the "enhanced" wave amplitudes, we obtain

$$P^+=\frac{1}{\sqrt{2}}\frac{\sin\theta}{\sigma^+(\theta)}(A_SA_{K0})^{\frac{1}{2}}\{\tfrac{1}{3}[\sin(\alpha_{33}-\alpha_3)+2\sin(\alpha_{33}-\alpha_1)]\},$$

$$P^0=\frac{\sin\theta}{\sigma^0(\theta)}(A_SA_{K0})^{\frac{1}{2}}\{\tfrac{1}{3}[\sin(\alpha_{33}-\alpha_3)-\sin(\alpha_{33}-\alpha_1)]\}. \tag{9-4}$$

These expressions should be especially valid for $\theta\simeq 90°$, since in this case, the smallness of the phase shifts other than α_{33} helps keep the contribution from "nonenhanced" P-wave terms small. The quantities A_S and A_{K0} appear in Eqs. (5-1).

In Fig. 14, we plot the expected polarization for $\theta\simeq 90°$, using Eqs. (9-4). As anticipated, this is small.

ACKNOWLEDGMENTS

We should like to express our appreciation to Professor M. Gell-Mann for his many suggestions and conversations relative to this paper.